

Load modulation strategies of residential heat pumps for demand-response programs with different thermal storage options

Emeline GEORGES^{1*}, Vincent LEMORT¹

¹Energy systems, Thermodynamics Laboratory, University of Liège,
Liège, Belgium

* Corresponding Author: emeline.georges@ulg.ac.be

ABSTRACT

This research work presents a methodology to assess the potential of load modulation strategies of HVAC systems for demand response programs at different scales. Two different demand response programs are considered: feed-in tariff signals for renewable production load matching and signals from the distribution grid operator for operational planning and congestion management at the distribution level. The resulting control problems are solved using optimal control formulations. First, the strategies are applied to four typical Belgian houses to match on-site PV production. Different thermal storage options are considered: on the one hand, thermal storage in the building envelope and in water tanks for domestic hot water, and, on the other hand, additional water tanks for space heating needs either in a parallel four-pipe or in a parallel two-pipe configuration. According to the type of house and the modulation strategy considered, a ranking of the most suitable storage options is proposed. Secondly, the method is extended to the scale of a distribution feeder with 50% PV penetration rate. Results show that with 20% heat pumps and suitable storage options, the residual load reduction reaches 28% to 73.4%. Upward load modulation in response to grid operator signals shows better performance for short modulation intervals, but can lead to up to 13% additional overconsumption if the chosen thermal storage option is not adapted to the house insulation level.

1. INTRODUCTION

The objectives of reduction of greenhouse gas emissions to mitigate the impact of human activities on global climate have highlighted the need for increased energy efficiency policies and energy transition towards renewable energy sources. The massive penetration of decentralized renewable energy sources and electrification of systems put additional stresses on the electricity grid and require changes in consumption profiles. As the building sector accounts for approximately 40% of the total energy demand in Europe, and with the increasing electrification of systems providing space heating (SH) and domestic hot water (DHW), such as heat pumps, there exists a large potential to control, enhance and adapt the related consumption profiles. In this context, there is a rising interest for demand response programs, which consist in the modification of consumption profiles in response to different incentives such as forward price signals, feed-in tariffs or direct signals from the grid operator. Several studies have focused on the potential of using the building thermal mass for load shifting. Results have shown that overheating the room temperature during off-peak hours can considerably reduce (by up to 20% according to Wolisz et al., 2013) the heating needs for the following peak hours. However, this leads to significant overconsumption (Reynders et al., 2013) and doesn't reduce peak demand amplitude but shifts in time (Masy et al., 2015). The use of DHW water tanks for demand response programs has also been investigated, for example, to reduce curtailing losses from PV panels in NZEBs neighborhood (De Coninck et al., 2014). The use of an extra water tank for space heating needs is less widespread in practice so far, but has been the interest of the several studies. Studies of Miara et al. (2014) and Palacio et al. (2014) focused on control strategies, and showed a possible reduction of up to 1.5% per every 10%

TES penetration of the overall power system's operation costs. Floss et al. (2015) studied the impact on the system performance of several hydraulic integrations (see Section 3.2) of SH thermal storages in heat pump driven heating systems. Hedegaard et al. (2012) compared the use of water tanks for SH to thermal storage in building structures for wind power integration. Finally, Patteeuw et al. (2016) propose an integrated approach to compare load shifting strategies with heat pumps to improve electricity generation efficiency at the system level. The present study compares two optimal control formulations for load shifting with residential heat pumps following a decentralized approach defined in Section 2. Three different storage options, presented in Section 3, are compared for four typical Belgian freestanding houses. A ranking of the most suitable option is presented in Section 4.1. In Section 4.2, the method is extended to a distribution feeder with 63 houses in order to reduce curtailment losses of PV production.

2. LOAD MODULATION STRATEGIES

This section proposes two optimal control formulations to trigger demand flexibility of residential buildings at a given time period and over set of consecutive periods. The load modulation amplitude is defined from a baseline profile that minimizes the electricity cost for the flexible consumer. The first formulation aims at activating an upward load modulation over a time interval. The second formulation aims at promoting load matching with local electricity production source over a given time interval by mean of a reduced electricity surplus selling tariff, as proposed by Georges et al. (2014).

2.1 Baseline consumption

The investigated system is represented by a discrete state-space formulation. The state transition is summarized by

$$x_{t+1} = f(x_t, u_t, w_t) \quad (1)$$

where x is the state space variable vector, u is the vector of decision variables, i.e. the modular electric power, and w is a vector of disturbances. The total electricity consumption of the consumer at time t , P_t^{cons} , is composed of modular components, $u_{i,t}$, i.e., the consumption of systems that can be adjusted by the optimal load management scheme, and the exogenous consumption, Γ_t , i.e. the share of the electricity consumption that is not modifiable,

$$P_t^{cons} = \sum_i u_{i,t} + \Gamma_t \quad (2)$$

A baseline consumption is obtained by minimizing the electricity costs for the flexible consumer for a given retail electricity price profile, π_{ret} ,

$$\min \sum_{t=1}^H (P_t^{cons} \pi_{ret,t}) \quad (3)$$

with respect to the decision variables, $u_{i,t}$, on the optimization horizon H , and subject to the following constraints

$$x_t^{\min} \leq x_t \leq x_t^{\max} \quad (4)$$

$$u_{i,t}^{\min} \leq u_{i,t} \leq u_{i,t}^{\max} \quad (5)$$

$$u_{i,t} + u_{j,t} \leq \max(u_{i,t}, u_{j,t}) \quad (6)$$

where Equation (4) specifies the upper and lower limits for power modulation of the modular components and Equation (6) ensures that two related decision variables are not activated simultaneously, as further explained in Section 3.3. The resulting baseline consumption profile is denoted \hat{P}^{cons} .

2.2 Upward modulation (ADR #1)

From the baseline consumption, a first mechanism can be implemented to trigger load flexibility in the desired time interval. It consists in carrying out an upward modulation of the electrical consumption at a given time period

τ over a number n of periods. The modulation profile, P_t^{mod} , is defined from the baseline consumption by the decision variable δ_t

$$P_t^{\text{mod}} = \hat{P}_t^{\text{cons}} + \delta_t \quad \text{for } t \in [\tau, \tau + n - 1] \quad (7)$$

The objective function is written as

$$\max(I_{\text{mod}}) \quad (8)$$

where

$$\delta_t \geq I_{\text{mod}} \quad \text{for } t \in [\tau, \tau + n - 1] \quad (9)$$

and subject to Constraints (4) to (6). After the n periods of upward modulation, a new consumption profile that minimizes the consumer's costs is determined as defined by Equations (3) to (6).

2.3 Load matching with buy-back ratio (ADR #2)

This optimal control formulation corresponds to a metering program that promotes load matching between production and consumption. The net electricity flow, P_t^{net} , i.e. the instantaneous difference between the power consumed and produced on site is determined. If positive, the billing tariff is the retail tariff, π_{ret} . If negative, the excess production is bought back at a buy-back tariff, π_{bb} . One can therefore define a buy-back ratio $\alpha_{\text{bb}} = \pi_{\text{bb}} / \pi_{\text{ret}}$. From a given time period τ and over n periods, the buy-back ratio is set to a value of zero. The objective is to minimize the electricity cost for the end-user for a given net metering buy-back ratio, which can be expressed as

$$\min \sum_{t=\tau}^H \left(\max(P_t^{\text{net}}, 0) + \min(P_t^{\text{net}}, 0) \alpha_{\text{bb},t} \right) \quad (10)$$

and subject to Constraints (4) to (6).

3. THERMAL MODELS

3.1. Buildings and Heat Pumps

Two types of building geometries, representative of the Belgian residential building stock, are considered in the study: a single-story building representative of freestanding houses built between 1971 and 1990 and a two-story building representative of freestanding houses built after 1991. For each geometry, two insulation levels are considered. Buildings characteristics are taken from the study of Gendebien et al. (2013) and summarized in Table 1. The building thermal behavior is modeled by an equivalent thermal network consisting of thermal resistances, R , in K/W, and lumped thermal capacitances, C in J/K. For the purpose of this study, two different single zone 5R3C models are used. They are illustrated in Figure 1. The first model structure (left), is used to model well-insulated buildings. The second structure (right), is a modification of the ISO13790 model (ISO, 2007) by the introduction of two additional lumped thermal capacitances to take into account the non-homogeneous air distribution in the zone and the thermal capacity of the internal walls. It is well-suited to model standard or poorly insulated buildings. Each building is equipped with an inverter air-to-water heat pump, whose characteristics are given in Table 1. The heat pump model is based on "ConsoClim" (Bolher et al., 1999) which expresses the heat pump coefficient of performance (COP) as a function of the ambient temperature, T_a , the water supply temperature, $T_{w,su}$ and the part-load ratio, PLR , through polynomial laws

$$COP = f(T_a, T_{w,su}, PLR) \quad (11)$$

Regression coefficients are identified based on performance curve from manufacturer data. The emitters installed in the building are conventional radiators. The emitted power is modeled with an empirical emission law function of the difference between the average water temperature in the emitter and the room temperature. The water supply temperature is adapted to the house insulation level and adjusted throughout the year following a heating curve.

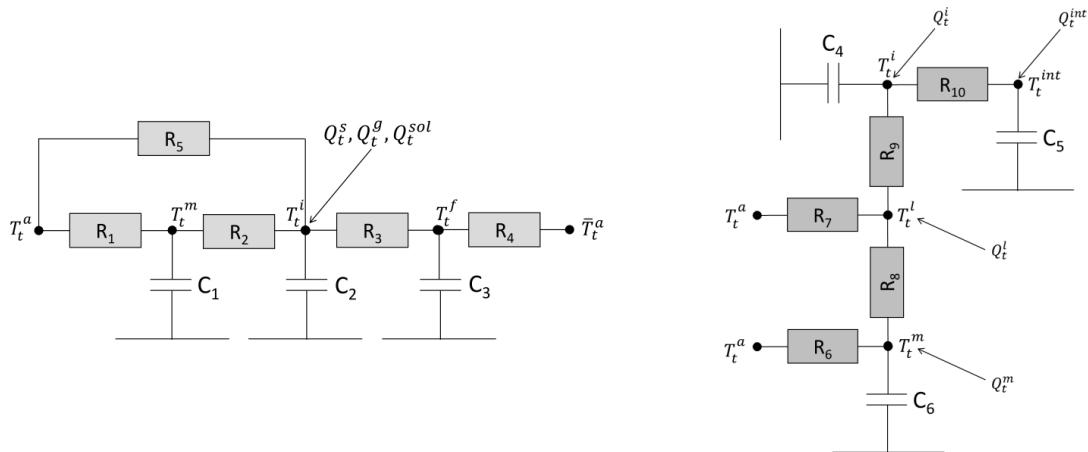


Figure 1: Grey-box model structures.

Table 1: Buildings and heat pumps characteristics

Year of construction	N# of floors	Heated volume [m ³]	Ground floor area [m ²]	Average U value [W/m ² K]	Design heat demand @ - 10°C [kW]	Nominal HP temperatures A/W [°C]	Auxiliary heater [kW]
2007-2014 (A)	2	457	75	0.31	6.5	7/45	3
1991-2006 (B)	2	457	75	0.46	8.0	7/45	3
1971-1990 (C)	1	423	148.5	1.24	17.0	7/65	5
1971-1990 (D) Retrofit	1	423	148.5	0.77	12.0	7/45	5

3.2 Thermal storage

Each house is equipped with a domestic hot water (DHW) tank. Additionally, three thermal storage options are investigated for space heating (SH):

- storage in the building envelope,
- storage in a water tank following the parallel four-pipe configuration (Figure 2 – right),
- storage in a water tank following the parallel two-pipe configuration (Figure 3).

As illustrated in Figure 2 (left), both storage tanks for SH and DHW are installed in parallel, and the heat pump can only supply one of them at a time. Priority is always given to the DHW tank. Both DHW and SH tanks are modeled by one-node models with homogeneous water temperature.

Table 2: Water storage tank volumes

House type	DHW tank Volume [m ³]	SH tank Volume [m ³]	SH Tank configuration
A1	0.25	/	/
A2		0.35	Two-pipe
A3		0.42	Four-pipe
B1		/	/
B2		0.40	Two-pipe
B3		0.52	Four-pipe
C1		/	/
C2		0.60	Two-pipe
C3		0.90	Four-pipe
D1		/	/
D2		0.50	Two-pipe
D3		0.75	Four-pipe

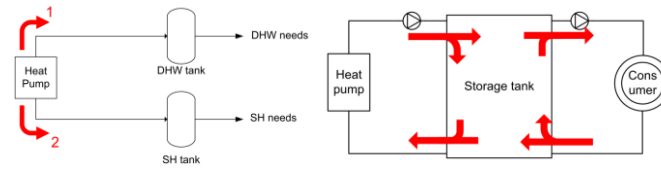


Figure 2: Left: Hydraulic scheme for DHW and SH water storages. Right: Parallel four-pipe configuration for SH water storage.

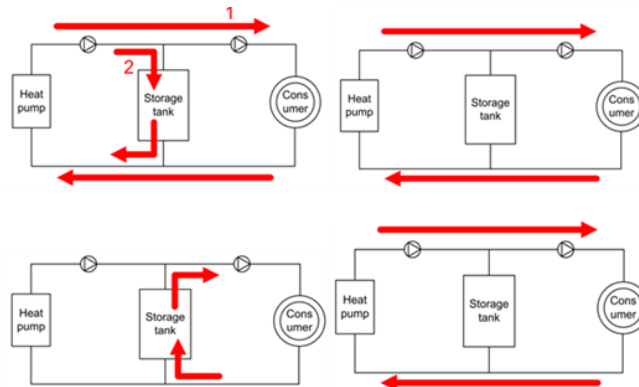


Figure 3: Parallel two-pipe configuration for SH water tank. Top left: the heat pump is used to supply the house directly if needed or to store heat in the storage tank. Top right: the heat pump is used to meet the house heating needs only. Bottom left: the storage tank, if charged enough, is used to supply the house. Bottom right: the storage tank charge level is too low to supply the house, and the heat pump is used to supply the house directly.

3.3 Constraints

Constraints (4) to (6) translate as follows, depending on the thermal storage option for SH:

- for thermal storage in building envelope, the building zone temperature, should remain within a dead band of ΔT equals 1K around the set point profile during occupancy hours and between the minimum and maximum daily set point for unoccupied hours. An intermittent heating strategy is chosen. The set point is set to 18°C during the night and unoccupied periods and to 21°C during occupied hours of the day.
- for the four-pipe SH tank configuration: the water temperature, T_{SH} , is always maintained above the house heating curve temperature, T_{hc} :

$$T_{hc} \leq T_{SH} \leq T_{hc} + \Delta T_{4-pipe} \quad (12)$$

where ΔT_{4-pipe} is set to 15K during grid-constrained periods, i.e. $[\tau, \tau + n - 1]$, and to 10K otherwise.

- for the two-pipe SH tank configuration: the water temperature has to be higher than the house heating curve temperature when the tank is used to supply the house, which corresponds to y_{SH} equals one:

$$T_{hc} y_{SH} \leq T_{SH} \leq T_{hc} + \Delta T_{2-pipe} \quad (13)$$

where ΔT_{2-pipe} is equal to 10K. The tank can only be supplied during grid-constrained periods.

- for both four-pipe and two-pipe configurations, the indoor temperature strictly follows the set point.
- the heat delivered to the house should not exceed the full load capacity of the heat pump and auxiliary heater combined or the limits imposed by the temperature in the tank and by the emission system.
- for DHW, the water tank temperature should remain within an imposed dead band:

$$50^\circ\text{C} \leq T_{DHW} \leq 57^\circ\text{C} \quad (14)$$

- the heat pump can only supply either the house, or the SH tank or the DHW tank at a time, which introduces Boolean variables and turns the optimization problem into a mixed-integer linear program.

4. RESULTS AND DISCUSSION

In this section, the two load modulation strategies ADR#1 and ADR#2 are applied to mitigate voltage fluctuations entailed by photovoltaic (PV) production in distribution networks. The objective consists in minimizing the residual load, i.e., the difference between the electricity production and consumption on a time interval $[\tau, \tau + n - 1]$. The strategies are first applied to each typical building A to D to compare the different storage options, and then extended to simulate the response of a set of buildings in a distribution feeder.

4.1 Influence of thermal storage options

Each association of house and thermal storage summarized in Table 2 is simulated for two typical winter days and one day in the spring. The activation takes place at time period 49 and the modulation lasts over 10 consecutive periods. The incentive signal for ADR #2 is illustrated in Figure 4 (left). Figure 5 illustrates the temperature and power consumption profiles obtained for simulations B1 to B3 for load strategy ADR#2 for a sunny winter day (Figure 4 - right). During the investigated time interval, the occupation profiles are such that there are no occupants in the house, and the allowed indoor temperature range is 17°C to 22°C. For all three storage associations, both DHW production and SH contribute to demand flexibility. During unoccupied periods, using thermal envelope for demand flexibility allows the best match with PV production. The power consumption modulation from the baseline reaches up to 3kW. Both the DHW tank and the zone can be preheated to meet comfort requirements imposed during occupied periods later in the day. With the parallel four-pipe configuration, most of the flexibility is provided by the SH tank. Its upper set point is raised by 5K to increase flexibility. Load matching is achieved during two concentrated time frames due to the limited storage capacity of both SH and DHW tanks and the limited heating demand of the house during unoccupied hours. The residual load, initially of 4.6 kWh for the baseline profile, is reduced by 47%. For the two-pipe configuration, load matching is ensured either by DHW production, or by direct space heating or by heat storage in the SH tank. The latter is mostly heated during the last periods of the interval. This is due to the fact that the house can only be supplied either by the SH tank or directly by the heat pump and also to the control strategy that anticipates the use of the SH tank later in the day. The residual load is reduced by 43%.

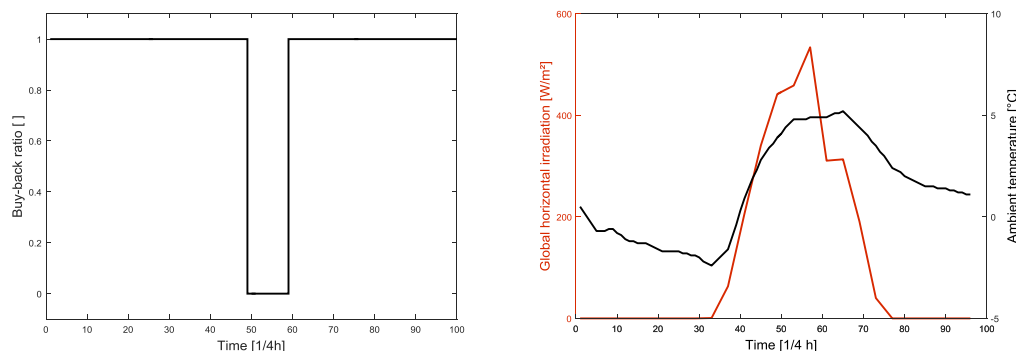


Figure 4: Global horizontal irradiation and ambient temperature for February 20th, 2012.

Figure 6 generalizes the findings of Figure 5 to houses A to D for the two control strategies. Results are presented in terms of average residual load reduction and additional overconsumption. The overconsumption is defined as the difference between the integrated daily electricity consumption of the baseline and the flexible profile. The additional overconsumption is the share of overconsumption that does not occur during the activation time interval. The determination of the most suitable storage option for each house depends on the criteria to satisfy. If the only objective is to reduce the residual load, heat storage in building envelope is the best option with both ADR#1 and ADR#2 for buildings A to D, due to the large storage capacity available. Residual load reduction reaches 51% to 85%. ADR#1 outperforms ADR#2 for poorly insulated houses such as C and D, whereas ADR#2 is more efficient for well-insulated houses such as A and B for which the good insulation of the envelope allows an efficiency use of

the stored heat. For ADR#1, the parallel two-pipe configuration allows an additional reduction of the residual load by 4% to 16% compared to the four-pipe configuration. This additional flexibility increases with decreasing house insulation levels. Indeed, for poorly insulated houses, the SH tank in the four-pipe configuration is often close to its highest temperature level at the beginning of the activation interval. For ADR#2, the difference in performance between the two-pipe and four-pipe vary strongly with the type of house. Indeed, for houses A and B, both storage options present similar ability to reduce the residual load. For houses C and D, contrariwise, trends are opposite. In the case of house C, the indoor temperature fluctuations induced by the supply of the SH tank reduce its potential to be used in a parallel two-pipe configuration, compared to better insulated houses such as D. If a condition regarding the overconsumption outside the modulation interval is added to the residual load reduction, then using thermal envelope as storage option becomes detrimental for house C for both ADR#1 and #2. The two-pipe configuration for houses C and D with ADR#1 also leads to significant overconsumption, as the energy stored in the tank may not be stored at a sufficient high temperature to supply the house afterwards. The four-pipe configuration becomes a suitable option for houses C and D.

4.2 Application to a semi-urban feeder

The methodology is applied to a typical semi-urban feeder in Belgium. The feeder has an average of 63 load points corresponding to 63 households, mostly composed of freestanding buildings (Gonzalez et al., 2012). Baetens (2015) has outlined the sensitivity of such feeders to high penetration of distributed generation sources and heat pumps. A penetration rate of PVs superior to 50% entails over-voltages, which could be reduced by load compensation. The four typical houses presented above are distributed in the feeder according to their share in the overall Belgian residential buildings stock. The number of inhabitants in each house is drawn from a normal distribution of average three and a standard deviation of two with a maximum of five occupants. The exogenous consumption profiles associated to lighting and appliances are obtained from article (Gendebien et al., 2015), as well as the domestic hot water draw-off events. It is assumed that the optimal controller knows the average demand profiles for all houses. Indoor temperature set points schedules are intermittent temperature profiles generated based on normal distribution laws for morning, midday and evening start-up times. All profiles have a weekly average indoor set point above 18°C. Occupancy profiles are derived from the latter. Simulations are run for both 10 and 20% of houses equipped with heat pumps. Based on the results from Section 4.1, the best suited storage option that satisfies both minimum residual load and minimum overconsumption is chosen for each of them. Additionally, 50% of the buildings are equipped with South, East or West-oriented PV panels with thirty-five degrees tilt angle and 18% average efficiency. The installed surface area is drawn from a discrete uniform distribution over an interval ranging from ten to forty square meters. Houses with PVs and heat pumps are distributed randomly over the 63 houses and their occurrence may not coincide. Load management strategies ADR#1 and ADR#2 are compared in Figure 7 for average exogenous consumption and domestic hot water profiles. For ADR#1, the input signal is to perform an upward modulation. For ADR#2, the same buy-back ratio as in Figure 4(left) is used, as well as the mean PV production per buildings. For a modulation interval located from period 49 to 58, ADR#1 and ADR#2 allows to reduce the peak residual power of period 57 from 63.1 kW with no heat pumps down 20.2kW and 30.1 kW with 20% heat pumps, respectively. The integrated residual load over the interval is reduced by 73.4% and 51.4% with ADR#1 and ADR#2 respectively, compared to no load modulation. The sensitivity in performance of ADR#2 to the PV production input used in Equation (10) is illustrated in Figure 8. If the modulation interval is extended from period 37 to period 71, and the input PV production provided to ADR#2 is the maximum PV production per house rather than the average production per house, then ADR#2 shows the best performance and provides an additional 23% reduction of the integrated residual load compared to ADR#1.

5. CONCLUSION

This paper proposes two optimal control formulations to compare load shifting strategies for residential heat pumps. Three storage options combining a DHW tank and either the thermal envelope of the building or a SH tank with two hydraulic configurations are investigated for four typical Belgian houses characterized by different insulation levels.

The method can be used to relieve network congestions, such as those caused by excess PV production. Results show that, for both control strategies, the use of the building envelope as storage option allows a reduction of the residual load by 51 to 75% for well-insulated houses. As the house insulation level decreases, different behaviors are observed according to the control strategy. To maximize the upward modulation while limiting overconsumption, the parallel four-pipe scheme is the most suitable, whereas the best load shaping is obtained with a parallel two-pipe or a parallel four-pipe configuration. At the scale of a distribution feeder with 63 houses, if 50% of the houses are equipped with PV panels, a penetration rate of 20% heat pumps with appropriate thermal storage allows to reduce the residual load by 28 to 73.4% depending on the control strategy and the modulation interval length. An upward modulation strategy shows good result for short interval lengths with relatively constant power production, whereas the load shaping strategy increases the residual load reduction by an extra 21% on longer intervals.

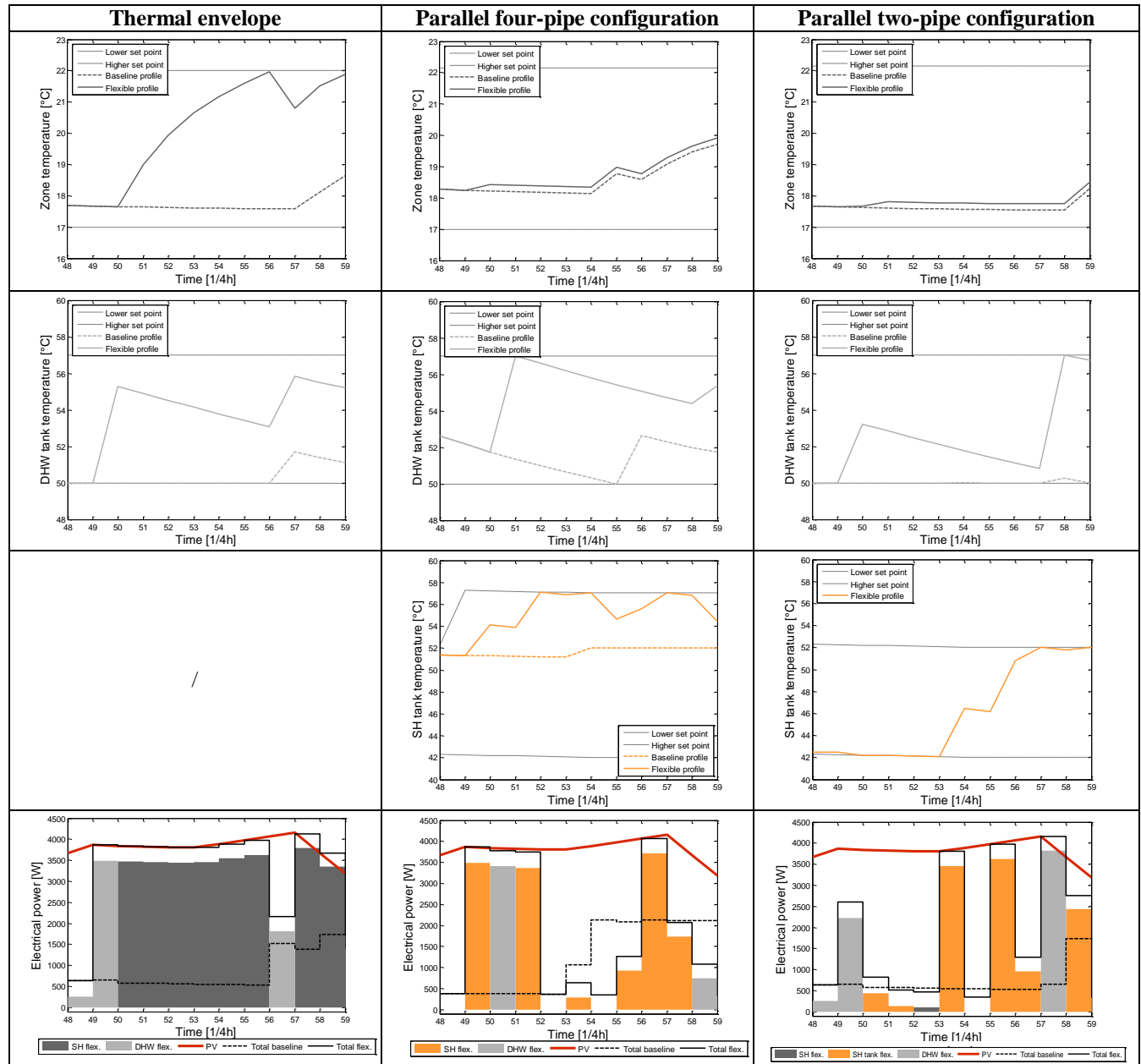


Figure 5: Illustration of load modulation formulation ADR#2 for house B and three thermal storage options for a winder day (Day 51 – February 20th).



Figure 6: Comparison of ADR#1 and ADR#2 for houses A to D and three storage options. Average values over two winter days and one day in the spring.

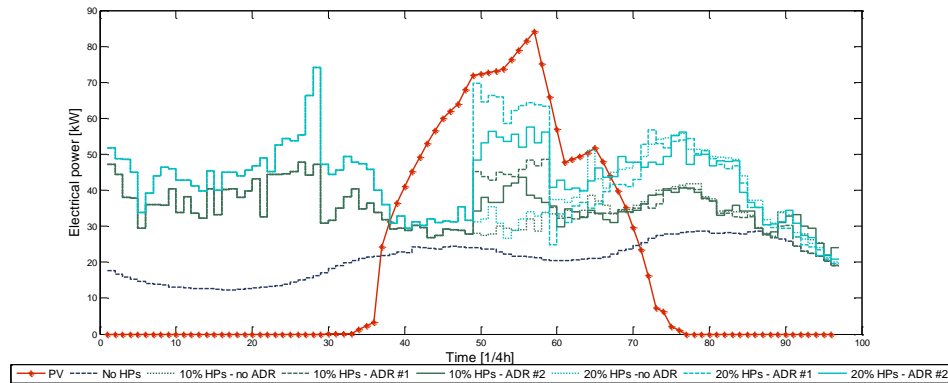


Figure 7: Load modulation strategies with 50% PVs and 10 and 20% penetration of heat pumps (HPs) for time period 49 to 58.

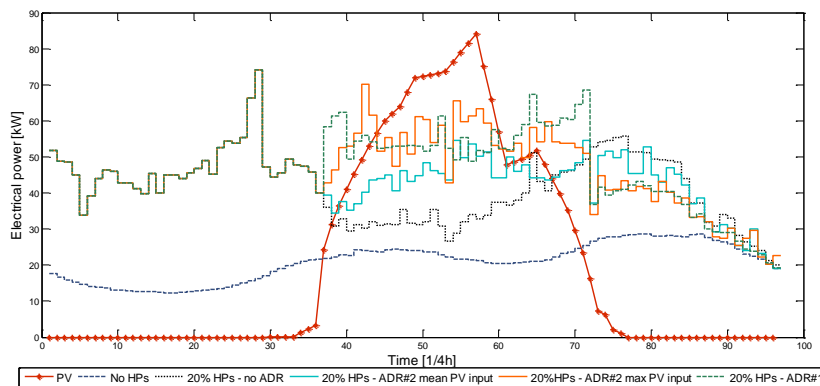


Figure 8: Impact of PV input for ADR#2 and of the modulation length on residual load reduction.

NOMENCLATURE

Q_i^g	Internal heat gains	Superscripts	
Q_i^{sol}	Solar gains	g	gain
T	Temperature	sol	solar
Q	Thermal power	s	space heating
Subscripts		i	indoor
t	at time t	m	massive
		l	light
		int	internal

REFERENCES

- Baetens, R. (2015). On Externalities of Heat Pump-based Low-Energy Dwellings at the Low-Voltage Distribution Grid. PhD dissertation, KUL, Belgium.
- Bolher A., Casari R., Fleury E., Marchio D.. (1999). Méthode de calcul des consommations d'énergie des bâtiments climatisés : ConsoClim. Technical report, Ecole des Mines (Paris).
- De Coninck, R., Baetens, R., Saelens, D., Woyte, A., & Helsen, L. (2014). Rule-based demand-side management of domestic hot water production with heat pumps in zero energy neighbourhoods. *Journal of Building Performance Simulation*, 7(4), 271-288.
- Floss, A., & Hofmann, S. (2015). Optimized integration of storage tanks in heat pump systems and adapted control strategies. *Energy and Buildings*, 100, 10-15.
- Gendebien, S., Georges, E., Bertagnolio, S., & Lemort, V. (2015). Methodology to characterize a residential building stock using a bottom-up approach: a case study applied to Belgium. *International Journal of Sustainable Energy Planning and Management*, 4, 71-88.
- Georges, E., Braun, J. E., Groll, E., Horton, W. T., & Lemort, V. (2014). Impact of net metering programs on optimal load management in US residential housing—a case study. *Proceedings of the 9th International Conference on System Simulation in Buildings (SSB2014)*, Liège, Belgium.
- Gonzalez, C., Geuns, J., Weckx, S., Wijnhoven, T., Vingerhoets, P., De Rybel, T., & Driesen, J. (2012). LV distribution network feeders in Belgium and power quality issues due to increasing PV penetration levels. *2012 3rd IEEE PES International Conference and Exhibition on In Innovative Smart Grid Technologies (ISGT Europe)*, (pp. 1-8). IEEE.
- Hedegaard, K., Mathiesen, B. V., Lund, H., & Heiselberg, P. (2012). Wind power integration using individual heat pumps—analysis of different heat storage options. *Energy*, 47(1), 284-293.
- International Standard Organization. (2007). ISO13790:2007: energy performance of buildings – calculation of energy use for space heating and cooling, Geneva, Switzerland.
- Masy, G., Georges, E., Verhelst, C., Lemort, V., & André, P. (2015). Smart grid energy flexible buildings through the use of heat pumps and building thermal mass as energy storage in the Belgian context. *Science and Technology for the Built Environment*, 21(6), 800-811.
- Miara, M., Günther, D., Leitner, Z. L., & Wapler, J. (2014). Simulation of an Air-to-Water Heat Pump System to Evaluate the Impact of Demand-Side-Management Measures on Efficiency and Load-Shifting Potential. *Energy Technology*, 2(1), 90-99.
- Palacio, S. N., Valentine, K. F., Wong, M., & Zhang, K. M. (2014). Reducing power system costs with thermal energy storage. *Applied Energy*, 129, 228-237.
- Patteuw, D., Henze, G. P., & Helsen, L. (2016). Comparison of load shifting incentives for low-energy buildings with heat pumps to attain grid flexibility benefits. *Applied Energy*, 167, 80-92.
- Reynders, G., Nuytten, T., & Saelens, D. (2013). Potential of structural thermal mass for demand-side management in dwellings. *Building and Environment*, 64, 187-199.
- Wolisz, H., Harb, H., Matthes, P., Streblow, R., & Müller, D. (2013). Dynamic simulation of thermal capacity and charging/discharging performance for sensible heat storage in building wall mass. In *Proceedings of Building Simulation Conference*.